JBC Papers in Press. Published on December 2, 2008 as Manuscript M806693200
The latest version is at http://www.jbc.org/cgi/doi/10.1074/jbc.M806693200

MEMBRANE HYPERPOLARIZATION DRIVES CATION INFLUX AND FUNGICIDAL ACTIVITY OF AMIODARONE

Lydie Maresova[1], Sabina Muend[2], Yong-Qiang Zhang[2], Hana Sychrova[1] and Rajini Rao[2#]
From the Departments of [1]Membrane Transport, Institute of Physiology, Academy of Sciences CR, Prague, Czech Republic and [2]Physiology, Johns Hopkins University School of Medicine, Baltimore MD, USA

Running Head: Hyperpolarization activated cation influx in yeast death

[#]Address correspondence to: Rajini Rao, Department of Physiology, Johns Hopkins University School of Medicine 725 N. Wolfe Street, Baltimore MD 21205 Phone: 410 955 4732; Email: rrao@jhmi.edu

Cationic amphipathic drugs, such as amiodarone, interact preferentially with lipid membranes to exert their biological effect. In the yeast *Saccharomyces cerevisiae*, toxic levels of amiodarone trigger a rapid influx of Ca^{2+} which can overwhelm cellular homeostasis and lead to cell death. To better understand the mechanistic basis of antifungal activity, we assessed the effect of the drug on membrane potential. We show that low concentrations of amiodarone (0.1-2 μM) elicit an immediate, dose-dependent hyper-polarization of the membrane. At higher doses (>3 μM), hyperpolarization is transient and is followed by depolarization, coincident with influx of Ca^{2+} and H^+ and loss in cell viability. Proton and alkali metal cation transporters play reciprocal roles in membrane polarization, depending on the availability of glucose. Diminishment of membrane potential by glucose removal or addition of salts or in *pma1*, *tok1Δ*, *ena1-4Δ* or *nha1Δ* mutants protected against drug toxicity, suggesting that initial hyper-polarization was important in the mechanism of antifungal activity. Furthermore, we show that the link between membrane hyperpolarization and drug toxicity is pH-dependent. We propose the existence of pH- and hyperpolarization activated Ca^{2+} channels in yeast, similar to those described in plant root hair and pollen tubes that are critical for cell elongation and growth. Our findings illustrate how membrane active compounds can be effective microbicidals and may pave the way to developing membrane-selective agents.

Antifungal drugs such as polyenes, azoles, allylamines and morpholines target differences between fungal and animal membranes. For example, azoles provide safe and effective fungistatic action by inhibiting the biogenesis of the fungal specific sterol, ergosterol. However, the development of secondary resistance to these drugs in the course of long-term therapy and the rising number of immunocompromised patients who fail to clear the trailing ends of fungal infection, has driven the search for new drugs that can augment the arsenal of antimycotics. Courchesne (1) reported that amiodarone, an ion channel blocker in clinical use as an antiarrhythmic agent, exhibited broad-range fungicidal effects at concentrations ranging from 5-15 μM. Gupta et al. (2) first demonstrated that the combination of 2-4 μM concentrations of amiodarone and azole drugs had a synergistic effect against *in vitro* growth of *Cryptococcus neoformans* and *Candida albicans* strains. Interestingly, azole resistant mutants in the ergosterol biosynthesis pathway of *S. cerevisiae* (*erg3Δ*, *erg6Δ*, *erg24Δ*) exhibited hypersensitivity to amiodarone, suggesting that the drug may be particularly effective for treatment against azole resistant fungal strains (2). This has been borne out by recent in vitro data of synergistic killing of azole resistant clinical isolates of *C. albicans* by amiodarone (3, 4). In light of these promising developments, we sought to understand the mechanistic basis for the fungicidal activity of amiodarone.

Multiple lines of evidence point to a role for drug induced calcium influx in mediating amiodarone toxicity. First,

amiodarone was shown to trigger a rapid, dose dependent calcium burst in yeast (2, 5), preceding mitochondrial fragmentation and cell death (6). A genome wide screen of yeast mutants revealed a correlation between some hypersensitive strains and defects in calcium handling (2); this included null alleles of Ca^{2+}-calmodulin regulated phosphatase calcineurin (*cnb1Δ*), Golgi/secretory pathway Ca^{2+}-ATPase (*pmr1Δ*), and vacuolar H^+ pump (e.g., *vma1Δ*) that provides the driving force for vacuolar Ca^{2+} sequestration. Transcriptional profiling of genes differentially regulated by amiodarone largely recapitulated the effects of calcium toxicity (7). Finally, modulation of the size and temporal kinetics of amiodarone-induced calcium transients, by altering metabolic status or extracellular calcium levels, elicited corresponding downstream effects in drug toxicity (8). Thus, chelation of extracellular Ca^{2+} with EGTA abolished the Ca^{2+} transient and protected against cell death; conversely, reintroduction of micromolar levels of Ca^{2+} to the depleted medium restored both calcium burst and amiodarone toxicity. Although these studies established a significant and causal role for Ca^{2+} influx in mediating drug toxicity, the mechanistic link between amiodarone and Ca^{2+} influx remained to be determined.

A starting point for the studies described herein was the observation that removal of glucose from actively growing cells had the immediate effect of attenuating amiodarone-induced Ca^{2+} burst and thus, protecting against drug toxicity (8). It is well known that H^+ pump activity of the yeast plasma membrane ATPase, Pma1, is immediately down regulated upon glucose removal (9), thereby coupling the electrochemical gradient across the membrane to energy levels in the cell. We hypothesized that the membrane potential may play a role in mediating the opening of Ca^{2+} channels and thus, fungicidal activity of amiodarone. Furthermore, depolarization of the membrane upon drug induced influx of Ca^{2+} and possibly other cations might contribute to cell death. Therefore, we investigated the effect of low doses of amiodarone on plasma membrane potential in wild type yeast, and in mutants with known perturbations of membrane potential. We show that a polarized membrane is critical for drug toxicity; furthermore, the change in membrane potential precedes and is closely coupled to both cation influx and cell death. Our findings offer insights into manipulation of membrane potential by a range of amphiphilic compounds that may be useful as antimycotic adjuncts or agents.

EXPERIMENTAL PROCEDURES

Media, Reagents, Strains and Growth

Yeast strains were grown at 30 °C in standard synthetic complete (SC) medium (Bio101 Inc., Vista, CA) or YPD. Stock solutions of amiodarone (Sigma, St Louis, MO) were 5 or 20 mM in DMSO. Stock solution of diS-C_3(3) (3,3'-dipropylthiacarbocyanine iodide) fluorescence probe (Molecular Probes) was 3 mM in ethanol. *Saccharomyces cerevisiae* wild type strain BY4742 (*MATα, his3Δ1 leu2Δ0 lys2Δ0 ura3Δ0*) was purchased from Invitrogen (Carlsbad, CA). Plasmid pEVP11-Aeq89 has been described (10). Other strains included W303-1A (*MATa ade2-1 can1-100 his3-11,15 leu2-3,112 trp1-1 ura3-1 mal10*; 11), TOW (*tok1Δ*; 12), BW31 (*ena1-4Δ nha1Δ*; 13), TOB (*ena1-4Δ nha1Δ tok1Δ*; 12). LMY69 (*HO arg6 PMA1*; Y55 306) and LMY65 (*HO arg6 pma1-105*; Y55 *arg6*; 14) were a kind gift from the laboratory of Wylie Nichols, Emory University, Atlanta, GA. Growth curves were measured in Elx808 BioTek reader as described earlier (15). For the drop tests, cells at an initial concentration of 0.5 $OD_{600\ nm}$ ml^{-1} were serially diluted in 3-fold increments and 2 μl aliquots were plated on YPD agar in Nunc omni trays. HP Scanjet 3570c was used to image the plates.

Monitoring of Membrane Potential Changes

The fluorescence assay for monitoring membrane potential changes was adapted from Denksteinova et al. (16) as follows: yeast cells

were inoculated into liquid YPD medium to the initial cell density of about 10^4 cells ml^{-1} ($OD_{600\ nm}$ ~ 0.001). The culture was cultivated for 8-15 h at 30 °C, till the cell culture reached exponential growth phase. The cells were harvested, washed twice with a citrate-phosphate (CP) buffer (10 mM Na_2HPO_4, citric acid to pH 6.0) and resuspended in the same buffer to $OD_{600\ nm}$ = 0.200 ± 5 %. The diS-C_3(3) fluorescence probe (0.1 mM working solution in ethanol) was added to 3 ml of yeast cell suspension to a final probe concentration of 0.2 μM. Salts (as indicated in the text) were dissolved in the CP buffer before addition of cells, amiodarone (from stock solution in DMSO) was added to the cell suspension in CP immediately after the fluorescence probe just before fluorescence measurement. Fluorescence emission spectra were measured on an ISS PC1 spectrofluorometer. The excitation wavelength was 531 nm, emission intensities were measured at 560 and 580 nm. The staining curves (i.e. the dependence of the emission intensity ratio (I_{580}/I_{560}) on the duration of staining t) were fitted as described (17) and the value of the intensity ratio at equilibrium was estimated.

Monitoring of Ca^{2+} Influx

The procedure was modified from Gupta et al. (2) as follows: 1 $OD_{600\ nm}$ of cells from overnight culture carrying pEVP11-Aeq-89 were spun down and resuspended in 50 μl SC media containing 0.75 μg of coelenterazine (Invitrogen, Carlsbad, CA) and incubated in the dark at 25 °C for 0.5 hour. The cells were washed twice with 2% glucose, resuspended in SC medium at 0.5 $OD_{600\ nm}$ ml^{-1}, and incubated at RT for 2.5 hr. 150 μl placed in each well of white, opaque 96-well plates. Luminescence was recorded using a BMG FLUOStar OPTIMA™ plate reader (BMG Labtechnologies Durham, NC). Total luminescence (L_{max}) was determined following lysis with 4% Triton X-100 (Fisher Scientific, Pittsburgh, PA) in 2 M $CaCl_2$. Free Ca^{2+} concentrations (in μM) were calculated as described in Gupta et al. (2).

External pH Measurements

Cells were washed three times with sterile distilled water and concentrated to 20 $OD_{600\ nm}$ ml^{-1}. 2 ml of concentrated cells were constantly stirred while the pH was recorded on Microsoft Excel 2003 every 10 seconds using an AccuFast pH electrode (Fisher Scientific, Pittsburgh, PA) connected to a PHM 92 Lab pH Meter from Radiometer Copenhagen (Brønshøj, Denmark). Glucose and amiodarone were manually injected to final concentrations specified in the figure legends.

Cytoplasmic pH Measurements

Cytoplasmic pH in yeast expressing pH-sensitive GFP, pHluorin, was determined by calculating the ratio of fluorescent intensity of emission at 520 nm with dual excitation at 410 nm and 485 nm, with calibration in media of defined pH, as described (18). Briefly, yeast cells transformed with plasmid pCB901YpHc (18) expressing cytoplasmic pHluorin were grown to late log phase ($OD_{600\ nm}$ ~4) in SC-Leu drop-out medium. Cells (200 μl) were spun down and resuspended in standard SC medium for 30 minutes and then transferred to clear-bottom black 96-well plates. Amiodarone was injected to desired concentration and fluorescence recorded on a BMG FLUOstar Optima multimode plate reader with accompanying BMG FLUOstar Optima Version 1.20-0 software (BMG Labtechnologies, Durham, NC). Where specified, cells were resuspended in SC medium adjusted to the indicated pH with NaOH, or resuspended in SC medium lacking glucose before amiodarone injection and fluorescence measurement.

RESULTS

Amiodarone Elicits Hyperpolarization of the Plasma Membrane

Fungal cells, like all eukaryotes, maintain inside-negative resting membrane potentials. Using microelectrodes, these membrane potentials have been measured to

reach values more negative than -180 mV in the filamentous fungus *Neurospora crassa* (19). Although measurement of absolute values of potential in smaller celled yeasts is more challenging and controversial (20), potentiometric probes provide reliable information on rapid changes in membrane potential (16). We used the potential sensitive fluorescence probe diS-$C_3(3)$ to monitor membrane potential changes in exponentially growing yeast cells, freshly resuspended in citrate phosphate buffer (pH 6.0). Low, micromolar concentrations of amiodarone caused dose-dependent increase in membrane potential, as seen by increased I_{580}/I_{560} emission ratio (red shift) of diS-$C_3(3)$ fluorescence from baseline values (Figure 1A). Figure 1B shows that the time course of hyperpolarization occurs within minutes of amiodarone addition. Addition of the protonophore CCCP effectively reversed the increased emission ratio, consistent with a collapse of the membrane potential. The rate of hyperpolarization was also dose-dependent; however, hyperpolarization was transient at higher doses (Figure 1C). Thus, at drug concentrations ≥4 μM, the I_{580}/I_{560} emission ratio decreased after 200 s suggesting that the membrane becomes depolarized. This decrease was accelerated by addition of CCCP (not shown), confirming that the observed fluorescence changes were related to changes in plasma membrane potential.

We investigated whether these changes in membrane potential were linked to drug toxicity. Yeast cells exposed to amiodarone under identical experimental conditions shown in Figures 1 A-C were plated and colonies counted to determine viability. Figure 1D shows that amiodarone concentrations that caused membrane depolarization also caused cell death. Thus, while hyperpolarization per se was not toxic, the subsequent depolarization phase correlated with drug induced loss of viability.

Role of Plasma Membrane H^+-ATPase in Glucose Medium

Glucose is known to increase membrane potential by increasing H^+ pumping activity of the plasma membrane ATPase, Pma1 (9). This is confirmed by a higher baseline I_{580}/I_{560} fluorescence ratio of diS-$C_3(3)$ in cells resuspended in citrate phosphate buffer supplemented with 2% glucose. Addition of amiodarone elicited a further increase in the membrane potential in glucose-supplemented yeast cells (Figure 2A). To investigate whether Pma1 activity contributed to drug induced hyperpolarization, a previously characterized mutant strain, *pma1-105* that has 65% reduction in activity (21), was compared to its isogenic wild type. In the absence of glucose, there was no difference in membrane potential between the mutant and wild type, both in the presence or absence of amiodarone (Figure 2B). This suggests that Pma1 has minimal activity in the absence of glucose. In contrast, in the presence of glucose, *pma1-105* was significantly depolarized relative to wild type and amiodarone-induced hyperpolarization was also lower. We conclude that Pma1 activity contributes to plasma membrane hyperpolarization by amiodarone, but only in the presence of glucose.

The higher level of hyperpolarization elicited by amiodarone in the presence of glucose correlates well with our previous observation of increased calcium burst and drug toxicity observed in glucose medium (8). If membrane potential increases were a necessary pre-requisite for subsequent cation influx, membrane depolarization and drug toxicity, we would predict that *pma1-105* yeast would be more resistant to amiodarone in the presence, but not absence of glucose. In the absence of drug, both *pma1* mutant and control strain show similar viability (Figure 2C; left panel). When amiodarone was added to cells in glucose containing medium for 10 minutes, *pma1* mutants showed increased survival relative to control (Figure 2C; right panel). This tolerance to drug was abolished when cells were incubated with amiodarone in the absence of glucose for ten minutes, prior to glucose addition and plating (Figure 2C; middle panel). The data of Figure 2 suggest

that amiodarone-induced hyperpolarization of the membrane is coupled to drug toxicity.

Role of Tok1 and Other Cation Transporters in the Absence of Glucose

Given the lack of effect of the *pma1-105* mutation on diS-C_3(3) fluorescence in the absence of glucose, we looked for other transport mechanisms that contributed to the observed drug-induced hyperpolarization. Tok1 is an outwardly rectifying K^+ channel that has been implicated in maintaining membrane potential (12). We show a lower resting membrane potential in *tok1Δ* in the absence of glucose (Figure 3A), as has been previously reported (12). Under these conditions, amiodarone-induced hyper-polarization was also reduced in the *tok1* mutant. However, in glucose containing buffer, there was no difference in membrane potential between *tok1* mutant and its isogenic wild type strain (Figure 3A), suggesting that Tok1 activity was reduced, absent or masked by Pma1 activity in the presence of glucose. These observations reveal a role for Tok1 in maintaining membrane potential specifically in the absence of Pma1 function.

It is evident from Figure 3A that in the absence of glucose, amiodarone can still elicit membrane hyperpolarization in the *tok1* mutant, indicating the contribution of additional transporters. The yeast strain BW31 (13) lacks all four *ENA* genes encoding plasma membrane Na^+ pumps, as well as *NHA1*, encoding the electrogenic plasma membrane alkali metal cation/H^+ antiporter. In the absence of glucose, resting membrane potential in BW31 was reduced, relative to wild type, and hyperpolarization in response to amiodarone was modestly decreased (Figure 3B). Deletion of *TOK1* in this mutant background further reduced resting membrane potential and amiodarone-induced hyperpolarization (Figure 3B). In the presence of glucose, however, none of these gene deletions altered membrane potential, either in the presence or absence of amiodarone (data not shown), as in the case of *tok1Δ* (Figure 3A). We conclude that together, Tok1 and other cation transporters are important for maintaining membrane potential in the absence of Pma1 function.

Further evidence linking membrane hyperpolarization to amiodarone toxicity was obtained by evaluating cell viability in the *tok1Δ* strain relative to wild type. Initial experiments with short incubation times failed to reveal statistically significant differences in dose response to amiodarone toxicity (not shown); however, following longer (overnight) incubation with 8 μM amiodarone, *tok1Δ* mutants exhibited significantly reduced lag times (and hence, increased viability) in the absence, but not presence of glucose (Figure 3C), consistent with results from drug induced membrane polarization. In the absence of amiodarone, both *tok1Δ* and wild type cells displayed similar growth characteristics (Figure 3C).

Depolarization by High Salt Blocks Amiodarone Toxicity

We have shown that single or multiple gene deletions that decrease membrane potential also have a protective effect against amiodarone toxicity. As an alternative approach to investigating the role of membrane potential in drug induced calcium influx and cell death, we evaluated the effect of high concentrations of salts known to depolarize the membrane. In Figure 4A, 100 mM concentrations of KCl, NaCl or $CaCl_2$ are shown to effectively reduce resting membrane potential. Under these conditions, amiodarone was unable to elicit significant hyperpolarization. Next, we evaluated the effect of high salt on amiodarone toxicity. Following 24 h growth, the minimal inhibitory concentration of amiodarone was between 5-10 μM, as reported previously (2). When added to cultures, KCl had a protective effect in the range 0.1-1 M (Figure 4B); with maximal protection observed close to the MIC. Thus, 100 mM KCl improved growth in 10 μM amiodarone from 5 to 60% of drug-free control. Previously, we showed that amiodarone toxicity is tightly coupled to

calcium influx (8). We hypothesized that the increased viability seen in the presence of high salt was due to decreased calcium influx. Amiodarone-induced calcium influx was evaluated by aequorin luminescence. As reported previously (2), low doses of amiodarone elicit a burst of calcium within minutes (Figure 4C-D). In the presence of 100 mM KCl, the calcium burst was both reduced and delayed; more complete abrogation of the calcium burst (Figure 4D) corresponded with increased protection from amiodarone toxicity (Figure 4B). Similar results were observed with 100 mM NaCl (not shown) and 100 mM $CaCl_2$ (8). We conclude that decreased resting membrane potential interferes with the ability of amiodarone to hyperpolarize the membrane, resulting in lower Ca^{2+} influx and consequently, increased viability.

Toxic Levels of Amiodarone Trigger H^+ Influx

Re-energization of yeast by glucose elicits a rapid and transient cytosolic acidification (22), followed by alkalinization upon activation of the plasma membrane H^+ pump, Pma1 (23). Given the hyperpolarizing effect of both glucose and amiodarone, we investigated whether drug exposure also elicited cytoplasmic acidification. As seen in Figure 5A, amiodarone caused an immediate and dose-dependent decrease in cytoplasmic pH, as measured by the ratiometric pH probe, pHluorin. Toxic levels of drug triggered significant (~0.4 pH unit) acidification of pH_{in} which failed to recover to resting levels, consistent with loss of metabolic activity and cell death (8). Further evidence for drug induced H^+ influx came from monitoring medium pH. It is known that glucose activation of Pma1 results in H^+ extrusion which can be monitored by decrease in pH_{out} (Figure 5B). Addition of toxic levels of amiodarone to glucose activated cells caused a dose-dependent alkalinization of pH_{out} (Figure 5B), consistent with cytoplasmic acidification seen in Figure 5A. The extent of medium alkalinization was proportional to the pH gradient across the cell membrane, with little or no alkalinization when the drug was added shortly after or before glucose addition. Thus, amiodarone elicited a large alkalinization of pH_{out} when added after maximal pH gradient was established (*trace 1*; Figure 5C). In contrast, the drug had no effect when added just before glucose (*trace 2*; Figure 5C), although a second addition after pH gradient formation elicited large alkalinization of pH_{out}. Addition of the drug at intermediate stages in pH gradient formation had intermediate effect (*traces 3,4*; Figure 5C). Consistent with a diminished effect of amiodarone on de-energized cells, we also observed no cytoplasmic acidification in cells resuspended in medium lacking glucose (Figure 5D).

These observations prompted us to examine the role of external pH in the cellular response to amiodarone. Amiodarone elicited a robust influx of H^+ (Figure 6A) and Ca^{2+} (Figure 6B) in SC medium (pH ~4.3) and in medium adjusted to pH 5 (not shown). Further small increases in external pH to 5.5-6 significantly reduced the extent of cytoplasmic acidification and Ca^{2+} burst. Essentially, no cation influx was observed at pH≥7. Concomittantly, cell viability was unaffected by drug at these alkaline pH (Figure 6B inset). Together, these findings point to a role for both Ca^{2+} and H^+ influx in mediating amiodarone toxicity. We note that the ability of drug to elicit membrane hyperpolarization was not diminished at higher external pH (Figure 6C). Thus, although amiodarone can interact with the membrane independently of external pH, a pH-dependent step activates cation influx and is essential for ensuing drug toxicity.

DISCUSSION

Reciprocal Roles of Proton and Alkali Metal Cation Transporters in Maintaining Membrane Potential

While it is well known that the plasma membrane H^+-ATPase, Pma1, is activated in glucose medium, our measurements of membrane potential reveal essentially no contribution by this ATP driven H^+ pump in

the absence of glucose, as seen by a lack of effect of the *pma1-105* mutation on both resting membrane potential and amiodarone-induced hyperpolarization. This tight regulation could be advantageous in conserving ATP in energy starved conditions. Instead, we show that in the absence of glucose, the outwardly rectifying K^+ channel Tok1 maintains the membrane potential (12), along with other cation transporters such as the $Na^+(K^+)/H^+$ antiporter Nha1 and the $Na^+(K^+)$-ATPases encoded by the *ENA* genes. Conversely, we could not detect significant contribution of Tok1, Nha1 and Ena transport systems to the membrane potential in glucose medium (not shown), suggesting a reciprocal role of these transporters in maintaining membrane potential. Electrophysiological recordings of Tok1 have shown outward K^+ currents at depolarizing potentials, likely to ensue in the absence of glucose and Pma1 function (24, 25). Upon hyperpolarization, the channel occupies multiple closed states, with increasing negative potentials trapping the channel in deeper inactive states. We note that the additive effect of multiple gene deletions on amiodarone-mediated hyperpolarization is consistent with the absence of any specific protein target; rather, our data suggest a general membrane-mediated effect as discussed ahead.

Cation Influx Channels Open upon Membrane Hyperpolarization

We show that membrane hyperpolarization by amiodarone correlates directly with drug toxicity. Thus, (i) increased hyperpolarization in glucose medium correlates with increased drug toxicity, (ii) attenuation of hyperpolarization by *pma1-105* mutation, or by *tok1Δ* and other gene deletions diminishes drug toxicity, and (iii) membrane depolarization by salts (KCl, NaCl or $CaCl_2$) also confers protection against amiodarone. Furthermore, we show that hyperpolarization is linked to, and likely precedes, calcium influx. Low (<1μM) concentrations of amiodarone cause membrane hyper-polarization in the absence of detectable levels of calcium or proton influx. Around 4 μM and higher drug concentrations, hyperpolarization is transient and rapidly reversed (Figure 1C), consistent with cation influx observed at these concentrations (2; Figure 4). These observations are reminiscent of earlier studies by Eilam and colleagues who monitored Ca^{2+} uptake in yeast as a function of increasing $\Delta\Psi$. Artificial increases of membrane potential, even in the absence of glucose, was seen to drive Ca^{2+} uptake suggesting that Ca^{2+} influx was mediated by channels which opened when $\Delta\Psi$ hyperpolarized to values more negative than a certain threshold (26). They further demonstrated that glucose addition to de-energized yeast caused transient cytoplasmic acidification, increased cAMP levels, and Ca^{2+} influx (27, 28). Taken together with our observations, we suggest that amiodarone elicits membrane hyperpolarization that drives cation influx. In this model, at amiodarone concentrations corresponding with growth toxicity, the resulting calcium and proton transients can overwhelm homeostatic mechanisms and lead to cell death (Figure 7). Hyperpolarization-activated, and low-extracellular pH dependent Ca^{2+} permeable ion channels have been described, although not yet cloned, in plant root hairs, pollen grains and tubes, where they are important in cell expansion and elongation (29, 30). Our studies predict the existence of similar channels in yeast, distinct from depolarization-activated ion channels, which could be potential drug targets.

Membrane Active Compounds are Effective Antifungals

As a cationic amphiphilic compound, amiodarone exhibits a very high partition coefficient (>10,000; 31) for lipid membranes, and has been reported to have an ordering effect on the fluid state of polar lipids (32, 33). It is well known that the physico-chemical composition of lipids modulates activity of membrane proteins, including pumps, channels and transporters, which could lead to the membrane potential changes and alterations in ion permeability described here. Alternatively, passive leak rates may be reduced by membrane ordering effects of the

drug. Future experiments could address the hypothesis that the microbicidal effects of amiodarone are mediated by its influence on the membrane bilayer, rather than by binding to one or few specific protein target(s), as in conventional drugs. Indeed, published (2) and ongoing studies (Zhang Y.Q. and Rao, R.; unpublished) with yeast mutants indicate that membrane lipid composition can modulate hypersensitivity or tolerance to amiodarone. Thus, amiodarone may be one of a growing number of compounds, including microbicidal peptides (*e.g.*, 34), which selectively disrupt target membrane function based on differences in lipid composition between host and pathogen. Understanding the basis of its fungicidal activity *in vitro* may lead to the development of more effective of drug combinations to combat life threatening fungal infections *in vivo*.

Acknowledgements

This work was supported by Czech grants MSMT LC531, AV0Z 50110509 to H.S., GA AS CR KJB500110701 to L.M., and by a grant from the National Institutes of Health R01AI065983 to R.R.

References

1. Courchesne, W. E. (2002) *J Pharmacol Exp Ther* **300**, 195-199
2. Gupta, S. S., Ton, V. K., Beaudry, V., Rulli, S., Cunningham, K., and Rao, R. (2003) *J Biol Chem* **278**, 28831-28839
3. Afeltra, J., Vitale, R. G., Mouton, J. W., and Verweij, P. E. (2004) *Antimicrob Agents Chemother* **48**, 1335-1343
4. Guo, Q., Sun, S., Yu, J., Li, Y., and Cao, L. (2008) *J Med Microbiol* **57**, 457-462
5. Courchesne, W. E., and Ozturk, S. (2003) *Mol Microbiol* **47**, 223-234
6. Pozniakovsky, A. I., Knorre, D. A., Markova, O. V., Hyman, A. A., Skulachev, V. P., and Severin, F. F. (2005) *J Cell Biol* **168**, 257-269
7. Zhang, Y. Q., and Rao, R. (2007) *J Biol Chem* **282**, 37844-37853.
8. Muend, S., and Rao, R. (2008) *FEMS Yeast Res* **8**, 425-431
9. Serrano, R. (1983) *FEBS Lett* **156**, 11-14
10. Matsumoto, T. K., Ellsmore, A. J., Cessna, S. G., Low, P. S., Pardo, J. M., Bressan, R. A., and Hasegawa, P. M. (2002) *J Biol Chem* **277**, 33075-33080
11. Wallis, J. W., Chrebet, G., Brodsky, G., Rolfe, M., and Rothstein, R. (1989) *Cell* **58**, 409-419
12. Maresova, L., Urbankova, E., Gaskova, D., and Sychrova, H. (2006) *FEMS Yeast Res* **6**, 1039-1046
13. Kinclova-Zimmermannova, O., Zavrel, M., and Sychrova, H. (2005) *J Biol Chem* **280**, 30638-30647
14. Stevens, H. C., and Nichols, J. W. (2007) *J Biol Chem* **282**, 17563-17567
15. Maresova, L., and Sychrova, H. (2007) *Biotechniques* **43**, 667-672
16. Denksteinova, B., Gaskova, D., Herman, P., Vecer, J., Malinsky, J., Plasek, J., and Sigler, K. (1997) *Folia Microbiol (Praha)* **42**, 221-224
17. Malac, J., Urbankova, E., Sigler, K., and Gaskova, D. (2005) *Int J Biochem Cell Biol* **37**, 2536-2543
18. Brett, C. L., Tukaye, D. N., Mukherjee, S., and Rao, R. (2005) *Mol Biol Cell* **16**, 1396-1405
19. Gradmann, D., Hansen, U.P., Long, W.S., Slayman, C.L., and Warncke, J. (1978) *J Membr Biol.* **39**, 333-67.
20. Ballarin-Denti, A., Slayman, C.L., and Kuroda, H. (1994) *Biochim Biophys Acta.* **1190**, 43-56.
21. Perlin, D. S., Harris, S. L., Seto-Young, D., and Haber, J. E. (1989) *J Biol Chem* **264**, 21857-21864
22. Ramos, S., Balbin, M., Raposo, M., Valle, E., and Pardo, L. A. (1989) *J Gen Microbiol* **135**, 2413-2422
23. Carmelo, V., Santos, H., and Sa-Correia, I. (1997) *Biochim Biophys Acta* **1325**, 63-70
24. Roberts, S. K. (2003) *Eukaryot Cell* **2**, 181-190
25. Vergani, P., Miosga, T., Jarvis, S. M., and Blatt, M. R. (1997) *FEBS Lett* **405**, 337-344
26. Eilam, Y., and Chernichovsky, D. (1987) *J Gen Microbiol* **133**, 1641-1649

27. Eilam, Y., Othman, M., and Halachmi, D. (1990) *J Gen Microbiol* **136**, 2537-2543
28. Eilam, Y., and Othman, M. (1990) *J Gen Microbiol* **136**, 861-866
29. Shang, Z.-L., Ma, L.-G., Zhang, H.-L., He, R.-R., Wang, X.-C., Cui, S.-J., and Sun., D.-Y. (2005) *Plant Cell Phys*. **46**, 598-608
30. Qu, H.Y., Shang, Z.L., Zhang, S.L., Liu, L.M., and Wu, J.Y. (2007) *New Phytol*.**174**, 524-536
31. Trumbore, M., Chester, D. W., Moring, J., Rhodes, D., and Herbette, L. G. (1988) *Biophys J* **54**, 535-543
32. Chatelain, P., and Laruel, R. (1985) *J Pharm Sci* **74**, 783-784
33. Rosa, S. M., Antunes-Madeira, M. C., Matos, M. J., Jurado, A. S., and Madeira, V. M. (2000) *Biochim Biophys Acta* **1487**, 286-295
34. Marx, F., Binder, U., Leiter, E. and Posci, I. (2008) *Cell. Mol. Life Sci*. **65**, 445-454
35. Herbette, L. G., Trumbore, M., Chester, D. W., and Katz, A. M. (1988) *J Mol Cell Cardiol* **20**, 373-378

Figure Legends

Figure 1: Amiodarone elicits dose-dependent hyperpolarization of the yeast plasma membrane

(A) I_{580}/I_{560} fluorescence emission ratio of diS-C_3(3) was measured in W303-1A wild-type yeast cells in CP buffer following addition of low doses of amiodarone (AMD) . Each column is an average of three independent experiments. (B) Fluorescence ratio was monitored in duplicate samples as in (A) following addition of the indicated doses of amiodarone (0, 0.5, 1 μM). The *arrow* indicates addition of protonophore (5 μM CCCP) to one sample of each duplicate pair. (C) diS-C_3(3) fluorescence ratio was monitored continuously following addition of the indicated concentrations of amiodarone (0.5-5 μM). Data are representative of three independent experiments. (D) W303-1A cells exposed to the indicated concentrations of amiodarone in CP buffer for 10 minutes were diluted 100-fold and plated on YPD medium. Colonies were counted to determine viability, relative to the starting cell density (100%). Data are representative of two independent experiments, average from triplicate colony counts are shown.

Figure 2: Amiodarone toxicity is linked to the membrane potential generated by Pma1 in glucose medium

(A) I_{580}/I_{560} emission ratio of diS-C_3(3) in wild-type LMY69 (WT) yeast resuspended in CP buffer in the presence (+) or absence (-) of 2% glucose and 0.4 μM amiodarone (AMD). Each column is an average of three independent experiments. (B) Comparison of membrane potential in isogenic wild type (LMY69; WT) and *pma1-105* mutant (LMY65; *pma1*) following treatment with 2% glucose and 0.4 μM AMD, as indicated. Each column is an average of three independent experiments. (C) Viability of WT and *pma1* yeast (0.5 OD_{600}/ml) was assessed on YPD agar following incubation in CP buffer supplemented with 2% glucose (left panel; control), or after exposure to 40 μM AMD in the absence (middle panel), or presence of 2% glucose (right panel) for 10 min. 3-fold serial dilutions from one of 2 independent experiments are shown.

Figure 3: Cation transporters maintain membrane potential in glucose-starved cells

(A) I_{580}/I_{560} emission ratio of diS-C_3(3) in W303-1A wild type (WT) and isogenic *tok1Δ* yeast in the presence (+) or absence (-) of 2% glucose and 0.4 μM of AMD, as indicated. Each column is an average of three independent experiments. (B) Additive effect of gene deletions on membrane potential changes upon addition of AMD (0, 0.2, 0.4 μM) in the absence of glucose. Isogenic WT, *ena1-4Δ*, *nha1Δ* and *tok1Δ* strains are shown. (C) Outgrowth of WT and *tok1Δ* yeast in YPD medium following overnight incubation in CP buffer supplemented with 2% glucose and 8 μM AMD as indicated. Following dilution of cells (1:20) into YPD, growth was measured periodically at $OD_{595\ nm}$. Data are representative two independent experiments.

Figure 4: Extracellular cations depolarize the membrane and diminish amiodarone toxicity

(A) I_{580}/I_{560} emission ratio of diS-C_3(3) in WT (W303-1A) in CP buffer supplemented as indicated with 100 mM concentrations of KCl, NaCl and $CaCl_2$ and 0.4 μM AMD. (B) Growth was monitored in the presence of AMD and KCl as indicated. Control (100%) growth was in SC medium in the absence of added salt or drug. Data are representative of two independent experiments. (C-D) Aequorin-coelenterazine luminescence in WT (BY4742) yeast was measured following injection of AMD (5 or 10 μM; *arrow*) in the presence or absence of 100 mM KCl. Data are average of triplicates and are representative of three independent experiments.

Figure 5: Amiodarone induces cytosolic proton influx and medium alkalinization

(A) Cytoplasmic pH was monitored using the fluorescent pH indicator, pHluorin, expressed in WT (BY4742) yeast. Fluorescence emissions (410/485 nm) ratios were measured in response to amiodarone addition (0-30 μM; *arrow*) and pH was calculated after calibration as described under *Experimental Procedures*. Data are averaged from three independent experiments. (B) Extracellular pH was monitored following addition of 2% glucose (*gray line*; Time 0). The *arrow* shows addition of amiodarone (10, 20, 30, 40 μM). Data are representative of 2 independent experiments. (C) The effect of a pH gradient on amiodarone-mediated alkalinization was monitored as in (B). Glucose was injected at *gray line* (Time 0); *arrows* indicate addition of amiodarone (10 μM). (D) Cytoplasmic pH derived from fluorescence emissions (410/485 nm) ratios as described in (A) were measured in response to amiodarone addition (0-30 μM; *arrow*) in the absence of glucose. Data are averaged from three independent experiments.

Figure 6: pH dependence of cation influx and amiodarone toxicity

(A) Cytoplasmic pH was monitored using pHluorin fluorescence as in Figure 5 (A), in WT (BY4742) yeast resuspended in SC medium adjusted to the indicated pH. Amiodarone (30 μM) or H_20 was injected into the cell suspension at the *arrow*. Data are the average of triplicate measurements. (B) Cytoplasmic Ca^{2+} was monitored using aequorin-coelenterazine luminescence in cells resuspended in SC medium adjusted to the indicated pH. Amiodarone (10 μM) was injected into the cell suspension at the *arrow*. Data are the average of triplicate measurements. (*Inset*) Viability was assessed in cultures (0.5 OD_{600}/ml) following incubation in SC medium adjusted to the indicated pH with amiodarone (40 μM) for 30 min, followed by serial three-fold dilutions on YPD agar. (C) Membrane potential was measured using diS-C_3(3) fluorescence as in Figure 1 (A) in CP buffer adjusted to the indicated pH, in the presence (+) or absence (-) or amiodarone (AMD; 0.4 μM). Strains with deletions in the indicated genes were evaluated.

Figure 7: Proposed mechanism of amiodarone toxicity

When added to cells maintained at resting membrane potential (*left*), amiodarone intercalates into the bilayer (35) and may alter lipid fluidity (33), resulting in membrane hyperpolarization (*center*). At higher doses, the membrane depolarizes as calcium and protons rush into the cytosol (*right*), disrupting ion homeostasis and leading to cell death.

Figure 1

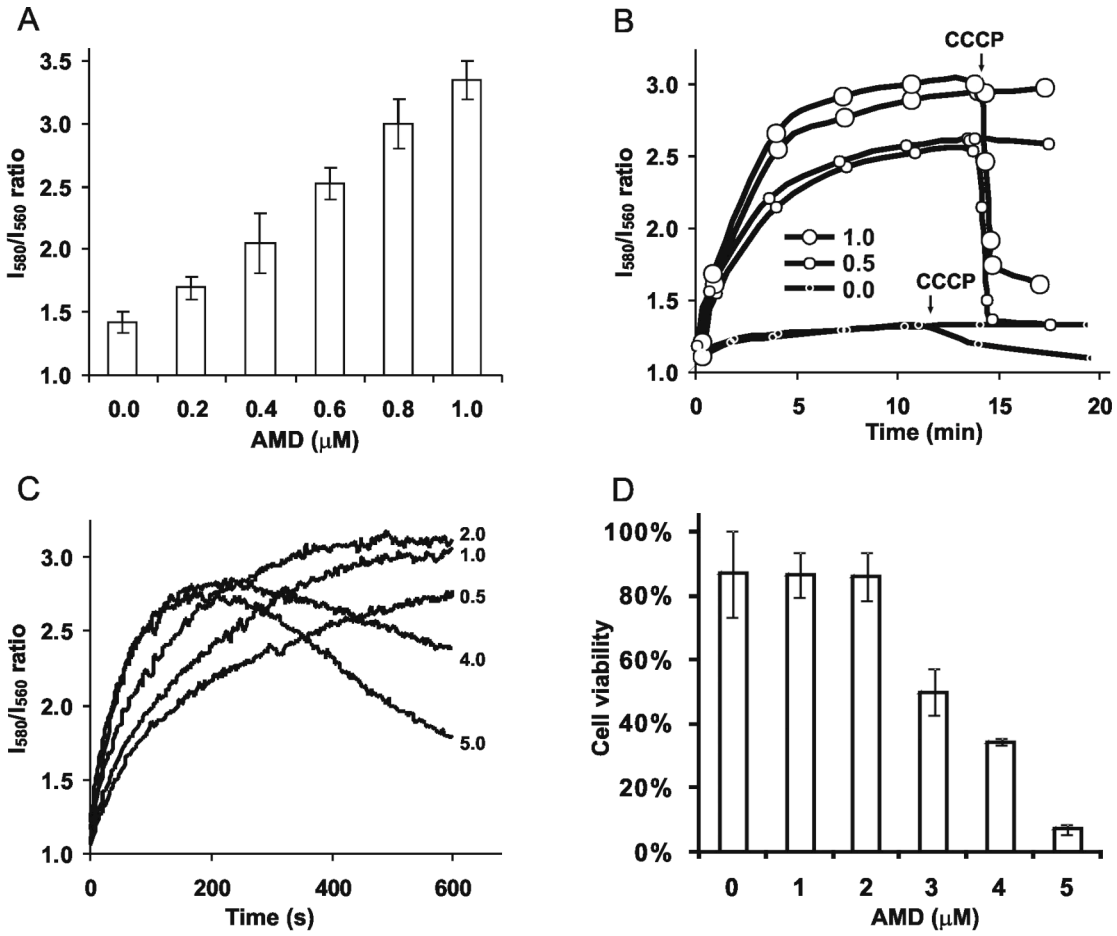

Figure 2

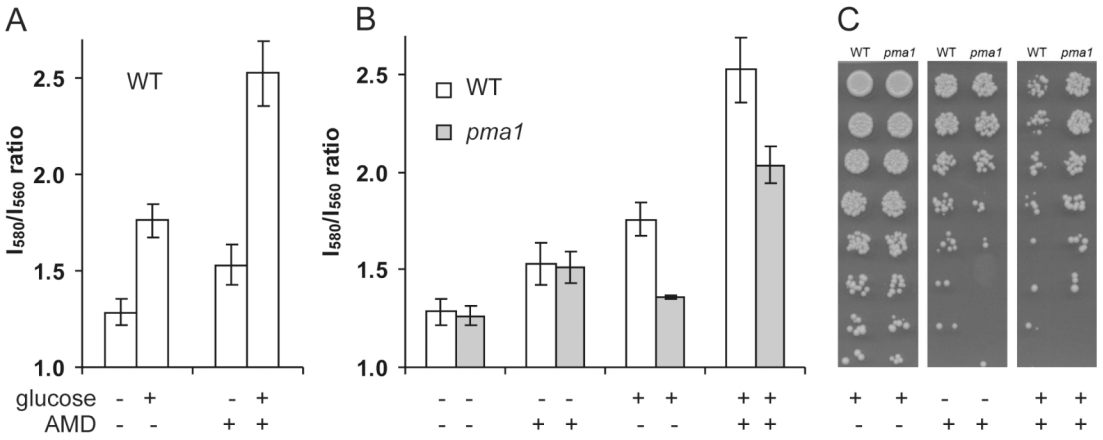

Figure 3

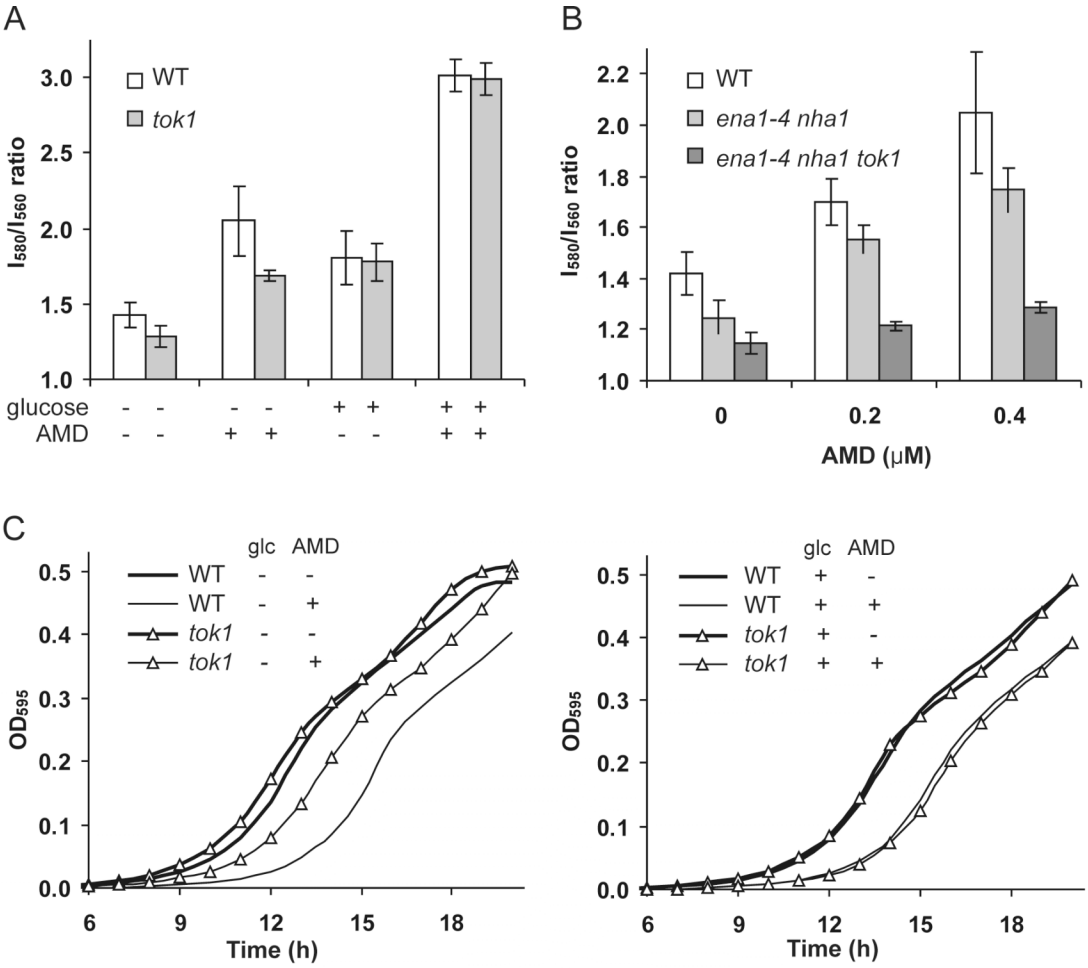

Figure 4

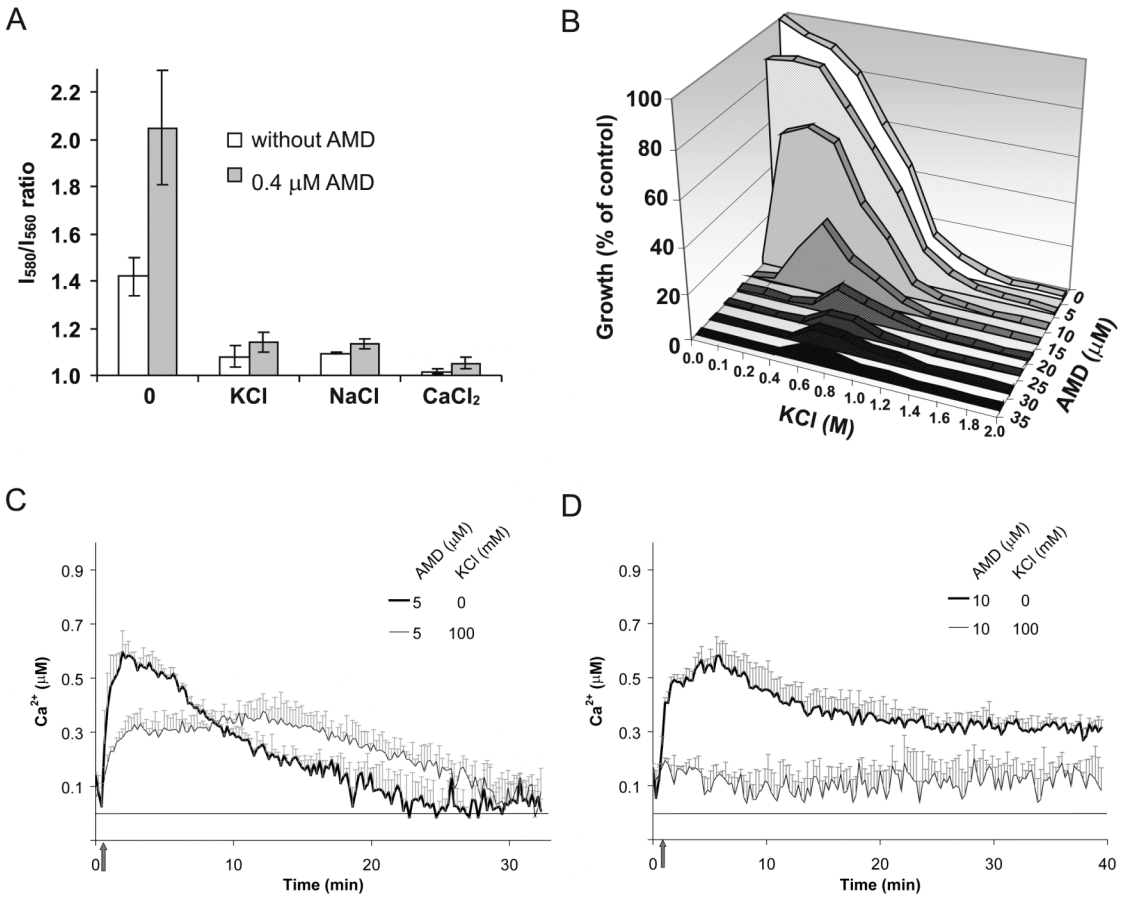

Figure 5

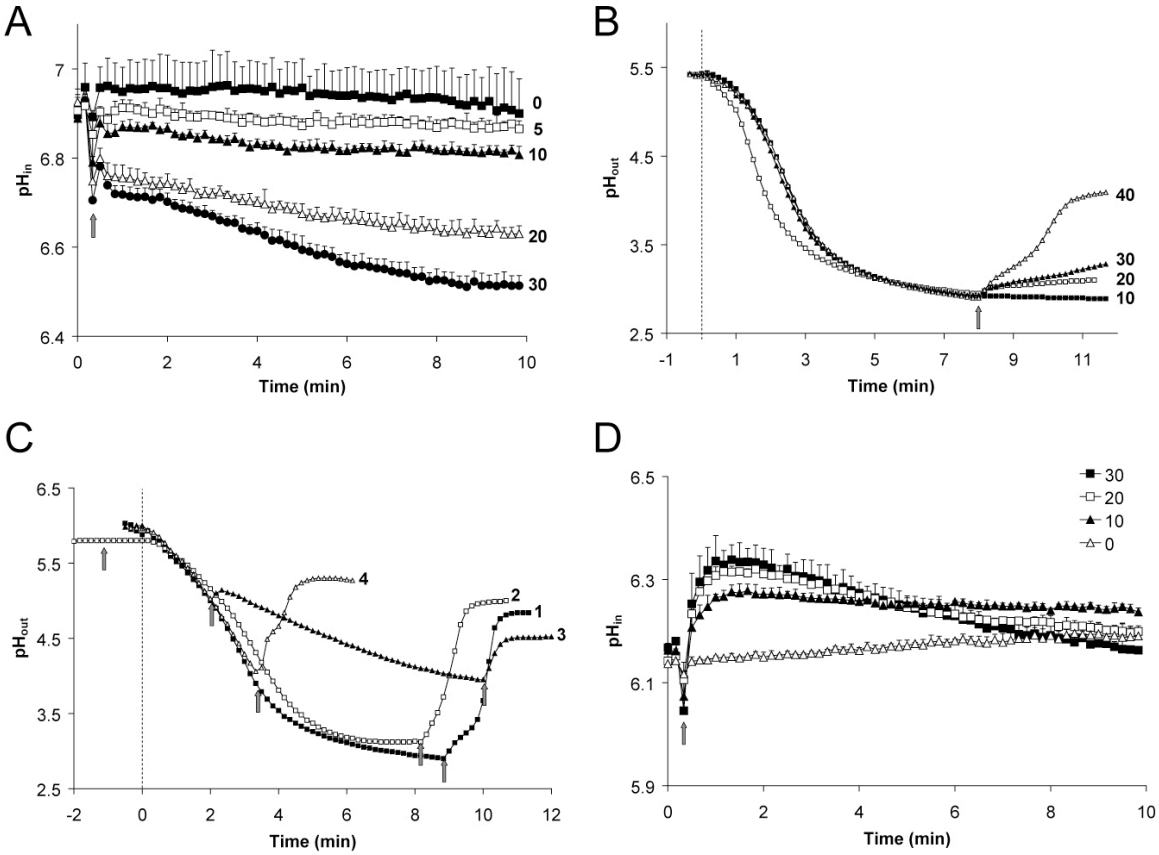

Figure 6

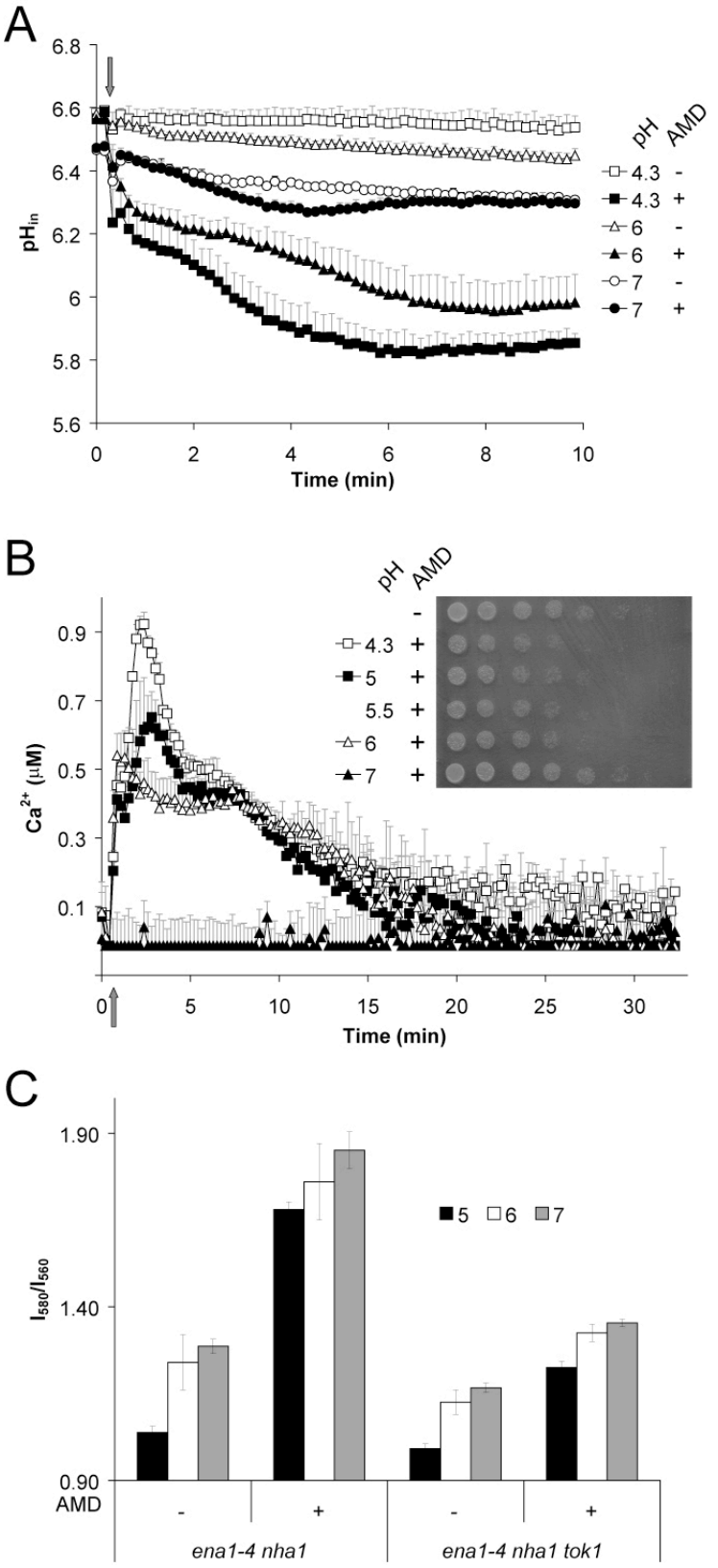

Figure 7